Evaluation of temperature-dependent adhesive performance via combinatorial probe tack measurements

Seung-ho Moon,[a] Arnaud Chiche,[b] Aaron M. Forster,[c] Wenhua Zhang, and Christopher M. Stafford[d]
Polymers Division, National Institute of Standards and Technology, Gaithersburg, Maryland 20899

(Received 15 November 2004; accepted 12 February 2005; published online 18 May 2005)

We describe the design and application of a temperature gradient probe tack apparatus for investigating the adhesive performance of model pressure-sensitive adhesives (PSAs). In particular, we illustrate a probe tack apparatus for studying the effect of temperature on three critical adhesion identifiers: adhesion energy, elongation at break, and debonding mechanisms. The measurement temperature is varied across the PSA film using a gradient temperature stage constructed from a transparent sapphire plate with a heating and cooling source positioned at opposite ends. The transparent substrate allows visualization of the contact area and debonding mechanisms during the test. The gradient temperature stage is integrated onto a motorized *x-y* stage, enabling a matrix of probe tack tests to be conducted across the PSA film at different sample temperatures. We use a spherical probe to evaluate the adhesive performance of a 150 μm thick model poly(styrene-b-isoprene-b-styrene) PSA film between a temperature range of 10 °C to 100 °C. We demonstrate that this apparatus is a viable combinatorial design for tack measurements and may be extended to more complicated two-dimensional gradient films. [DOI: 10.1063/1.1906105]

I. INTRODUCTION

Pressure-sensitive adhesives (PSAs)[1,2] are a class of soft adhesives that are able to adhere to a surface by applying light contact pressure and short contact times, without a chemical reaction or solvent evaporation. This particular behavior originates from the ability of the material to create intimate conformal contact with a stiff surface (liquid behavior), along with a concomitant capacity to sustain a significant load before failure of this contact occurs (solid behavior). To achieve these properties, PSAs are typically soft, viscoelastic polymers that are well above their glass transition temperature (T_g) and, at times, display moderate crosslinking.

There exist several methods for testing the adhesive strength of PSAs, including tack, peel, and shear tests. Although not as common as traditional peel tests, probe-type tack tests provide deeper understanding of the adhesive behavior and failure modes in PSAs. First described by Wetzel[3] in 1957, probe-type tack tests consist of bringing a rigid probe of known geometry into and out of contact with a flat adhesive layer while recording the applied displacement and resulting force throughout this cycle. Originally, only the maximum tensile force applied during probe separation was measured and subsequently converted into a nominal stress using the probe surface area.[4] In the 1970s, several studies of fracture in macroscopically elastic media highlighted the importance of the energy dissipated locally during crack propagation.[5–7] Following these fundamental discoveries, researchers began to measure the energy required to fully detach the probe from the PSA layer, which consequently transformed the tack setup.[8] However, quantitative predictions of the amount of energy dissipated during the process have always failed due to a lack of knowledge of the mechanisms involved in the separation process.

During the 1980s, Zosel[9] examined the complete evolution of the applied tensile stress during separation of the probe from the adhesive. The nonlinear behavior of the load-displacement curve highlighted the existence of several mechanisms occurring during the debonding of soft adhesives. This observation led Zosel to attach a video camera to his apparatus that was focused on the edge-on view of the probe/substrate interface.[10] By doing this, he could directly observe the formation of a complex and heterogeneous stretched structure at the later stages of debonding, which he interpreted as a fibrous network of adhesive material bridging between the probe and the film. As a result, the occurrence of a plateau in the measured stress at the end of probe-type tack tests has been originally designated "fibrillation."

More recently, Creton, Shull, and co-workers studied the micro-mechanisms involved in adhesive debonding using real-time observation through the adhesive substrate. This improvement allowed them to show that the debonding of an adhesive film is initiated by the growth of cavities in the bulk of the film[11] or by fingerlike crack propagation either in the bulk or at the interface with the probe.[12] The mode of failure is responsible for the initial stress peak and depends on the adhesive confinement,[13] mechanical properties,[13] and the ad-

[a]Present address: R & BD Center, Samsung Corning Co., LTD, Suwon-Si, Korea 443-732.
[b]Present address: Physikalische Chemie II, Universität Bayreuth, D-95440 Bayreuth, Germany.
[c]Present address: Multifunctional Materials Branch, United States Army Research Laboratory, Aberdeen Proving Ground, Maryland 21005.
[d]Author to whom correspondence should be addressed; electronic mail: chris.stafford@nist.gov

herent surface physico-chemistry.[14] It follows that the "fibrillation" is in fact related to the stretching of a two-dimensional open- or closed-cell foam (depending on the initial stages of the debonding process).

Today, probe-type tack experiments remain the focus of many research groups, both academic and industrial. The evolution of the technique has advanced the understanding of adhesive bond performance through additional knowledge gained from improvements in equipment,[15,16] increased complexity of test protocols,[17–19] and continuous integration of additional measurements during a single test.[20] A natural progression in the evolutionary development of probe-type tack tests is the integration of combinatorial and high-throughput (C&HT) approaches in order to develop a deeper understanding of adhesive performance and failure. C&HT methods combine experimental design, instrument automation, and computing tools to form a new paradigm for scientific research, where arrays or libraries containing continuous or discrete changes in one or more parameters enable multivariant screening of material properties. Recently, Grunlan *et al.* reported[21] a high-throughput approach for screening PSA libraries having variations in adhesive thickness and composition. They dispensed an array of adhesive formulations onto a transparent plastic substrate, and probe-type tack measurements were performed (in series) using a single spherical probe test. Conversely, the multilens contact adhesion test (MCAT)[22,23] is another platform for studying the interfacial properties of adhesives in parallel. Instead of a single probe, an array of hemispherical probes is brought into and out of contact with a flat sample. Although the measurement scheme for MCAT is highly parallel, the force acting on each individual lens is not measured and thus conventional tack curves cannot be generated. A review of various combinatorial approaches to measuring polymer adhesion has been published.[24]

Since PSA performance is strongly influenced by the viscoelastic behavior of the adhesive, the role of test temperature is very important. For example, with the increase of the experimental temperature, the viscosity of PSAs decreases and thus tack strength may increase due to more intimate contact between the adhesive and substrate, especially if the probe has some degree of surface roughness. Simultaneously, it may also lower the cohesive strength of the adhesive layer. Therefore, adhesive behavior as a function of temperature is quite a complicated issue warranting more detailed investigation. For any temperature study, the instrument should be designed carefully. The entire setup should be enclosed in a temperature-controlled chamber or a hot/cold stage should be properly designed. Furthermore, measurements must be started when the target temperature has reached steady state. If a single sample is used for a series measurements at different temperatures, additional experimental error might be anticipated since the sample must be aged at each temperature and thus the material properties might deviate from their original state. If multiple samples are employed, differences among the samples can increase overall measurement uncertainties. For those reasons, a new high-throughput approach to probe-type tack tests would be attractive since overall measurement time is decreased as well as consecutive measurements are performed on a single test specimen.

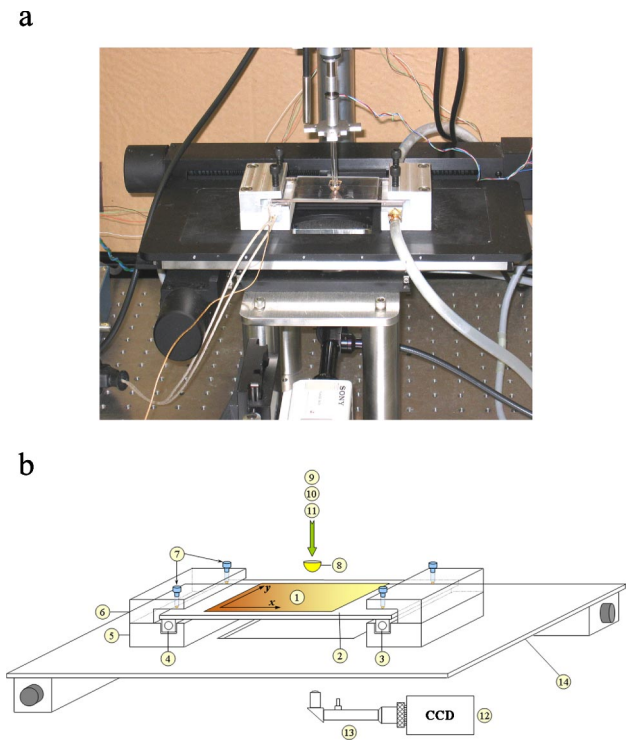

FIG. 1. (Color online) Combinatorial probe tack design: (a) a labeled photo of high-throughput probe tack test, (b) a schematic of the custom-built instrument: (1) sample, (2) sapphire window, (3) cooling, (4) heating, (5) PTFE block, (6) aluminum block, (7) screw, (8) glass probe, (9) piezoelectric nanopositioner, (10) load sensor, (11) displacement sensor (12) camera, (13) optics system, and (14) motorized *x*-*y* stage. A temperature gradient was maintained across the sapphire plate on which sample was placed. Motion of the *z*-actuator as well as data acquisition was controlled by a desktop computer (not shown).

In this article, we detail the design, construction, and application of a combinatorial probe-type tack apparatus with an integrated temperature gradient stage. This instrument is an efficient screening tool for understanding the adhesive properties of PSAs as a function of temperature as well as other critical parameters. To demonstrate our instrument, we perform measurements on a model PSA system consisting of a triblock copolymer of styrene-isoprene-styrene (SIS) and an added tackifier. The adhesive film is fully transparent and there is a substantial effect of temperature on the adhesive properties of SIS. Force-displacement profiles and contact images are acquired across the gradient in temperature, providing key information related to adhesive performance.

II. EXPERIMENTAL SETUP AND OPERATION

A. Instrument design

A schematic of our custom-built probe tack apparatus is shown in Fig. 1. Each component in the figure is labeled with a number for clarity, and a short description and discussion of each component is listed below. A PSA film (1) is either applied directly to a sapphire window (2) or separately cast onto a glass slide that is then anchored to the window. Sapphire was chosen for both its good thermal conductivity

($k_{\text{sapphire}}=35\ \text{Wm}^{-1}\,\text{K}^{-1}$, $k_{\text{glass}}=1.4\ \text{Wm}^{-1}\,\text{K}^{-1}$, $k_{\text{aluminum}}=216\ \text{Wm}^{-1}\,\text{K}^{-1}$, all at 293 K) and optical transparency. The temperature gradient is applied along the *x* axis of the specimen. A second gradient can be applied along the *y* axis of the specimen (e.g., film thickness, probe velocity, dwell time). The temperature gradient is achieved by positioning cooling (3) and heating (4) channels at opposite ends of the sapphire window. The heating channel in our design is $\frac{1}{4}$ in. (6 mm) diameter and holds a 175 W cartridge heater. The cooling channel is also $\frac{1}{4}$ in. (6 mm) diameter and is either filled with a second cartridge heater or plumbed for chilled water regulated by a conventional recirculating bath. The heating and cooling sources are set into machined polytetrafluoroethylene (PTFE) blocks (5) to thermally isolate the temperature gradient from the *x*-*y* translational stage. The sapphire window is held in place by a complimentary pair of aluminum blocks (6) and nylon-tipped screws (7) for thermal isolation.

Probe-type tack measurements are conducted by bringing a hemispherical glass probe (8) into and out of contact with the PSA film. Vertical displacement of the probe is controlled by a piezoelectric nanopositioner (9) (IW-812 Inchworm, Burleigh Instruments, Inc.).[25] The motion of the nanopositioner is controlled via software routines (e.g., LabVIEW) to govern loading/unloading speed, maximum displacement or load, and dwell time. An inline load sensor (10) (ELFM [25 N max], Entran Devices, Inc.) monitors the applied force while the absolute displacement is measured by a fiber optic displacement sensor (11) (RC62, Philtec, Inc.). Since glass has a very low thermal expansion coefficient ($\alpha_{\text{linear}}=0.5\times10^{-6}$), we may assume that thermal expansion of glass rod and probe is negligible within our experimental conditions. The importance of including a glass rod spacer will be further discussed in following section. The contact area between the probe and surface during approach and retraction is monitored by a digital camera (12) (DXC-390, Sony Corp.) and associated optics system (13) (Infinistix-Plus, Edmund Optics, Inc). Magnification and working distance of the optic system are tailored simply by specifying a power module amplifier (4×), a main body (1.5×,94 mm) and an objective (1×). This results in 6× total magnification. Since the sample and heating/cooling block are integrated onto a motorized *x*-*y* stage (14), probe-type tack tests are conducted sequentially across the temperature gradient. Data acquisition is coordinated by a host computer through an I/O connector block (SCB-68, National Instruments, Inc.) in conjunction with a data acquisition card (NI PCI-6024 E, National Instruments) and a custom-designed program. Load and displacement data as well as images were sampled at a speed of 5 points/s.

B. Temperature calibration

The temperature stage was constructed using a heat source on one side and a heat sink on the other side, and a linear temperature gradient is achieved by adjusting the endpoint temperatures. LabVIEW was used to monitor and record the temperature along a series of thermocouples (K-type) placed on the surface of the sample on the sapphire window. The thermocouples were connected to the PCI board through a SCB-68 board. Each channel is specified by

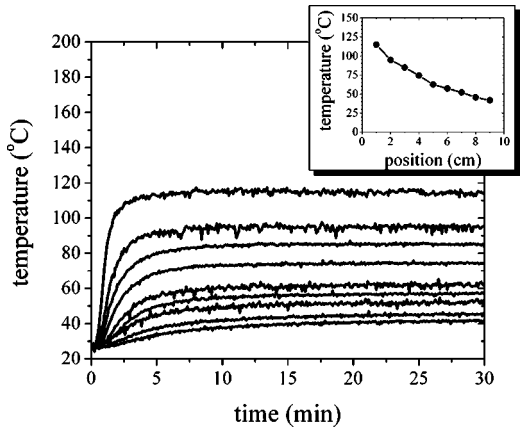

FIG. 2. Plot of the surface temperature as a function of position along the specimen. The gradient was generated by heating one end of the sapphire window to 150 °C while the other end was held at 25 °C. Inset: Temperature profile along the *x* axis of the specimen measured at 30 min after heating. The error bars represent one standard deviation of the data, which is taken as the experimental uncertainty of the measurement. Some error bars are smaller than the symbols.

LabVIEW. We wrote an acquisition program by modifying the "Continuous Thermocouple Measurement" LabVIEW subroutine (VI) to simultaneously convert thermocouple voltages into temperature values. Data collection speed was 10 points/s. When the heater and cooler temperatures were set to 150 °C and 25 °C, respectively, the temperature reaches steady-state values within 30 min, as shown in Fig. 2. The inset shows the temperature profile along the *x* axis of the specimen measured at 30 min after heating, and a nearly linear temperature gradient could be observed. Since the spacing between thermocouples was 1 cm, the gradient in temperature was approximately 1 °C/mm.

One issue of this test geometry is the sensitivity of the load sensor to the near surface temperature of the gradient specimen, which we observed to be quite significant. The load cell output drifts as the probe approaches to the hot surface. Shown in Fig. 3 is the measured drift in the load cell output (△) as the temperature gradient stage is brought up to an elevated temperature and subsequently cooled. It should be noted that the glass probe was held close to, but not in contact with, the temperature stage while acquiring the data plotted in Fig. 3. In order to alleviate this drift, we added a 4 cm long 5 mm diameter glass rod ($k_{\text{glass}}=1.4\ \text{Wm}^{-1}\text{K}^{-1}$ at 293 K) as an insulator between the load cell and probe. With this addition, the instability of load cell with temperature was reduced dramatically (• in Fig. 3), and drift-free load-displacement curves were acquired. Therefore, the load cell must be insulated from large temperature swings to obtain reliable load displacement curves, as shown in Fig. 4(a).

C. Data acquisition and analysis

Next, we describe the operation of our probe tack device by using measurements on a model PSA. A commercial grade of SIS triblock copolymer (Vector 4111, Dexco Polymers) was used as the polymer matrix for the model adhesive blends, and an aliphatic C5 hydrocarbon resin (Escorez 5380, Exxon Mobil) was chosen as the tackifier. The composition investigated here was 40% mass fraction polymer with

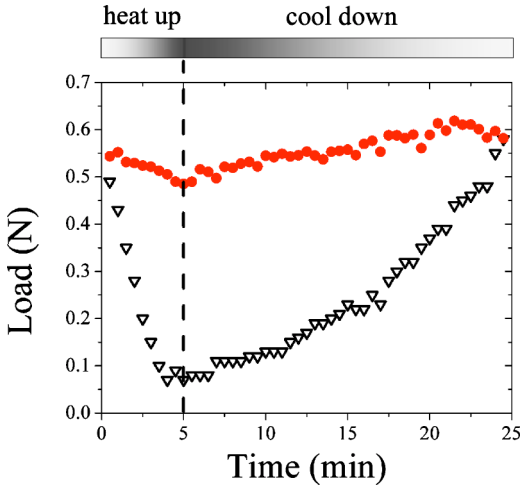

FIG. 3. (Color online) Drift of the load with surface temperature (△: without insulator, ● : with insulator). It should be noted that the probe is close to the surface but not directly in contact (convective heat transfer).

60% mass fraction of tackifier. The samples were prepared by solution casting onto 75×50 mm^2 glass microscope slides. A 15% mass fraction polymer blend solution was prepared by stirring the mixture in toluene for 24 h. Films were cast at room temperature in air for 24 h followed by vacuum drying at 60 °C for 24 h. Films thickness was approximately 150 μm, determined by gravimetrics. We chose this thickness because it is within the range used by adhesive tape manufacturers and is similar to that found in the literature.[26–28] Films prepared in this way were fully transparent.

Adhesive films were placed onto the temperature gradient stage and allowed to reach thermal equilibrium for 30 min. After reaching equilibrium, tack was measured serially. A hemispherical glass probe with a radius of curvature of 5 mm was used for the measurement to avoid the critical issue of probe-film alignment. The probe was brought into contact with the PSA film until a maximum load of 1.5 N was reached, at which point the probe was retracted until complete removal of the probe from the adhesive film was attained. Both the loading and unloading velocities were 2 μm/s, and dwell time at maximum load was 1 s. Images of contact area were obtained throughout the loading/unloading cycle. Five measurements were conducted along a line of constant temperature (y axis, orthogonal to the gradient). These measurements were spaced every 10 mm along the x axis. The testing matrix provides five repeatability measurements approximately every 5 °C. Since we are bringing an ambient temperature probe into contact with a heated adhesive film, the exact temperature at the interface between the adhesive film and the glass probe is not known. However, the heat transfer between the glass probe (insulator) and the adhesive film (insulator) should be minimal for the typical contact time (3 min) required. If one wanted to account for this disparity in temperature, the probe could be outfitted with a separate heating element, but this would significantly increase the experimental time due to the need to equilibrate the probe at each temperature along the gradient. Between each measurement the probe was cleaned with a lint free cloth soaked in toluene, dried, and cooled to room temperature via natural convection.

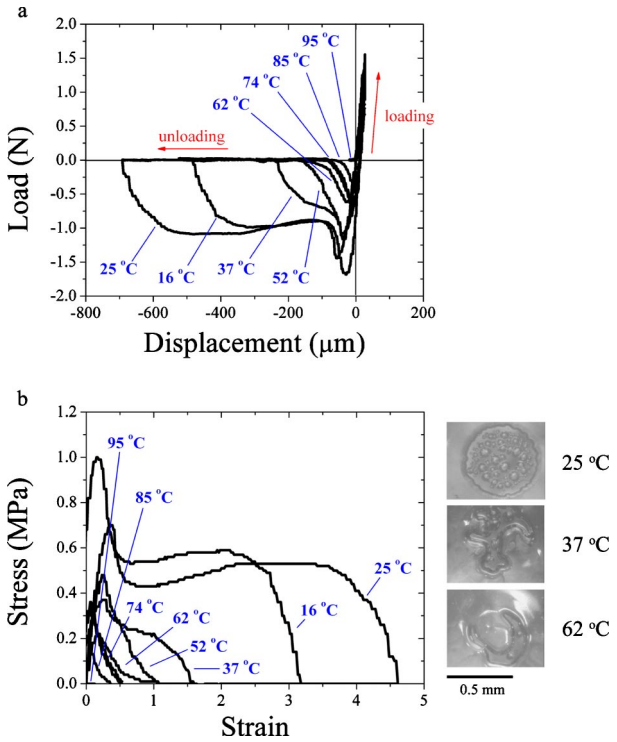

FIG. 4. (Color online) (a) Load-displacement and (b) stress-strain curves measured at several positions (different temperature) for a SIS-based adhesive. Stress is normalized by maximum contact area and strain is normalized by film thickness. Loading/unloading velocity, maximum load, and dwell time are 2 μm/s, 1.5 N, and 1 s, respectively. Contact images in (b) are obtained during the debonding stage (plateau) of the stress-strain curve.

III. EXAMPLE AND DISCUSSION

Figure 4(a) presents force-displacement curves for our model PSA system, obtained along the temperature gradient (x axis) of the sample. Although force-displacement curves can be directly used to evaluate adhesive properties by measuring initial peak height, area under the curve, or displacement of the probe prior to debonding,[22] it is useful to further analyze these strain-stress curves to better understand the mechanical behavior of the adhesive films.[9] The stress normalized by maximum contact area (σ) and strain normalized by initial film thickness (ε) were calculated to permit comparison of tack measurements at different locations on the PSA film. Here, $\sigma=F/(\pi\cdot a_{\max}^2)$ and $\varepsilon=d/h$, where F, $a_{\max}$, d, and h are force, maximum contact area, displacement, and initial thickness of the film, respectively. In Fig. 4(b), the nominal stress versus strain curves are shown for temperatures of 16, 25, 37, 52, 62, 74, 85, and 95 °C. The maximum value of the contact radius, $a_{\max}$, ranges from 0.5 mm at 25 °C to 0.7 mm at 95 °C, therefore the $a_{\max}/h$ ratios vary from 3.3 at 25 °C to 4.6 at 95 °C. This is a consequence of conducting maximum compressive load controlled tests, compared to displacement controlled tests.

There are two temperature-dependent trends evident from Fig. 4(b). The first is the maximum tensile force decreases with increasing temperature, as shown also in Fig. 5(a). This behavior has been demonstrated for flat probe tack

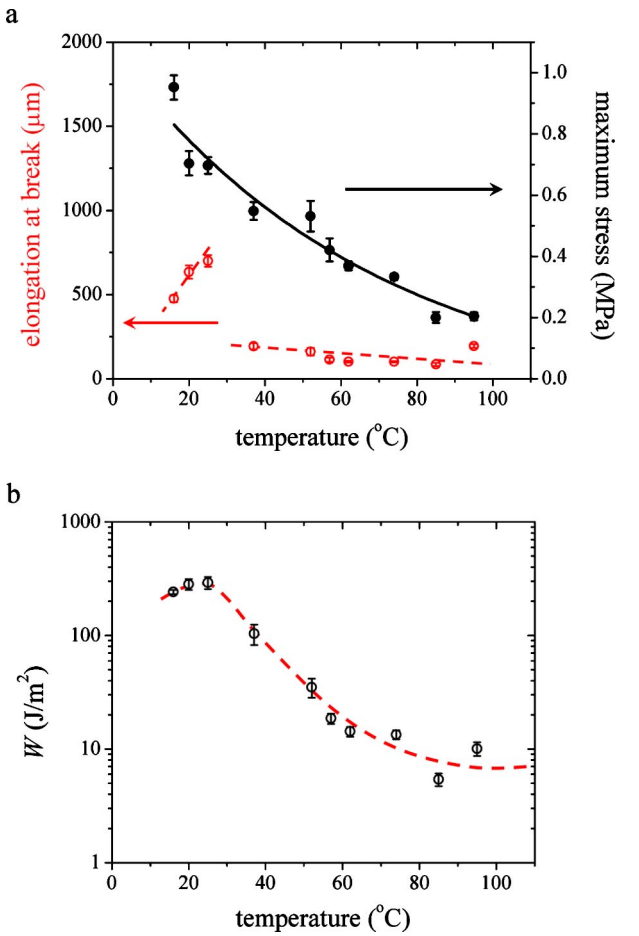

FIG. 5. (Color online) (a) Elongation at break and maximum stress along with (b) adhesion energy as a function of temperature (dashed lines serve as a guide to the eye). The error bars represent one standard deviation of the data, which is taken as the experimental uncertainty of the measurement. Some error bars are smaller than the symbols.

tests on similar PSA systems.[28] The decrease in maximum tensile force with increasing temperature is related to the drop in modulus of the polymer film at higher temperature. The second trend concerns the fibrillation step. Below 37 °C, the curves exhibit a notable plateau. The elongation at break, corresponding to the length of this plateau, increases with increasing temperature as shown in Fig. 5(a) (slope $\approx 0.06\ ^\circ C^{-1}$). Above 37 °C, the plateau has nearly disappeared and separation of the adhesive from the probe occurs suddenly after the initial stress peak. The elongation at break is then much smaller than for lower temperatures and tends to decrease as the temperature increases [Fig. 5(b)]. This transition in the stress versus strain curve shapes can be understood through the images taken from the contact after the initial stress peak, shown in Fig. 4(b). At 25 °C and below, cavitation occurs within the adhesive, leading to a stable foam that undergoes significant deformation via stretching (fibrillation). At 37 °C, we start to see external crack propagation (fingering) during the fibrillation (middle picture). This fingerlike crack propagation becomes dominant at higher temperatures. There is no more fibrillation and the elongation at break decreases (slope $\approx -0.01\ ^\circ C^{-1}$) as the viscous behavior of the material increases.

We can now consider the temperature dependence of the total adhesion energy W [Fig. 5(b)], calculated from the area under the force-distance curve divided by maximum contact area. This energy presents a maximum value around 25 °C. Indeed, below this temperature, the maximum stress decreases with increasing temperature but the elongation at break increases, favoring fibrillation as the major mechanism of energy dissipation and results in a slight increase in total adhesion energy. Above 25 °C, both the magnitude of the initial peak and the elongation at break decrease with increasing temperature, thus the adhesion energy decreases tremendously [note the logarithmic scale in Fig. 5(b)].

One interesting finding is the special behavior that has been observed at 95 °C, which is near the glass transition temperature of styrene block. Elongation at break displays an increase at 95 °C [Fig. 5(a)] and thus the debonding energy appears to reach a plateau [Fig. 5(b)]. It is believed that irreversible deformation may result in higher total adhesion energy.[29] SIS adhesives have a relatively high and constant value of E' but exhibit decreased loss properties such as tan δ at high temperature,[27] implying that bulk energy dissipation processes during debonding become a dominant factor in overall adhesive performance. During the debonding process, failure occurs either at the probe-surface interface or inside the adhesive layer, which can be described by a thermodynamic balance between the work of adhesion and the cohesive energy. Although studying the detailed mechanism of debonding is not the primary purpose in this paper, cohesive failure seems to be more favorable at higher temperature, especially near the PS glass transition temperature (T_g of bulk PS $\approx 100\ ^\circ C$).

We have demonstrated the ability to conduct combinatorial and high-throughput adhesion measurements of PSAs by using a probe-type tack instrument combined with a gradient heating stage. Although tack tests were conducted in a serial manner across the temperature gradient, our design yields a dramatic decrease in the total measurement time to adequately survey the entire temperature range studied. For example, adhesion measurements at ten different temperatures by conventional tack tests would take 10× (30 min equilibration at each temperature +3 min for tack test) =330 min, while adhesion measurements using the temperature gradient tack apparatus would take 30 min equilibration on temperature gradient +10× (3 min for tack test) =60 min. Thus, by incorporating a temperature gradient stage, we realize more than a 5× increase in measurement throughput. We believe this new high-throughput technique has considerable analytical utility because several critical pieces of information can be acquired simultaneously and more efficiently. In this paper, we presented only one-dimensional *in situ* tack measurements, opting to use the second dimension to conduct multiple identical tests for statistical purposes, but further applications are available. For example, combinatorial aging tests and kinetic studies of epoxy curing can be examined using this instrument. By introducing another parameter such as aging or curing time, 2-D libraries (e.g., time and temperature) can be easily generated and screened by probe-type tack measurements.

ACKNOWLEDGMENTS

Contribution of the National Institute of Standards and Technology, not subject to copyright in the United States. AMF and CMS acknowledge the NIST National Research Council Postdoctoral Fellowship Program. We thank Peter L. Votruba-Drzal and Michael J. Fasolka for insightful discussions and helpful comments.

[1] I. Benedek and L. J. Heymans, *Pressure-Sensitive Adhesives Technology* (Marcel Dekker, New York, 1997).
[2] A. Paiva, N. Sheller, M. D. Foster, A. J. Crosby, and K. R. Shull, Macromolecules **34**, 2269 (2001).
[3] F. H. Wetzel, ASTM Bull. 221, 64 (1957).
[4] F. H. Hammond, ASTM Bull. 360, 123 (1964).
[5] A. N. Gent and J. Schultz, J. Adhes. **3**, 281 (1972).
[6] E. H. Andrews and A. J. Kinloch, Proc. R. Soc. London, Ser. A **332**, 385 (1973).
[7] D. Maugis and M. Barquins, J. Phys. D **11**, 1989 (1978).
[8] R. Bates, J. Appl. Polym. Sci. **20**, 2941 (1976).
[9] A. Zosel, Colloid Polym. Sci. **263**, 541 (1985).
[10] A. Zosel, J. Adhes. **30**, 135 (1989).
[11] H. Lakrout, P. Sergot, and C. Creton, J. Adhes. **69**, 307 (1999).
[12] K. R. Shull, C. M. Flanigan, and A. J. Crosby, Phys. Rev. Lett. **84**, 3057 (2000).
[13] A. J. Crosby, K. R. Shull, H. Lakrout, and C. Creton, J. Appl. Phys. **88**, 2956 (2000).
[14] C. Creton, J. Hooker, and K. R. Shull, Langmuir **17**, 4948 (2001).
[15] B. A. Francis and R. G. Horn, J. Appl. Phys. **89**, 4167 (2001).
[16] S. Poivet, F. Nallet, C. Gay, and P. Fabre, Europhys. Lett. **62**, 244 (2003).
[17] G. Josse, P. Sergot, C. Creton, and M. Dorget, J. Adhes. **80**, 87 (2004).
[18] R. E. Webber and K. R. Shull, Macromolecules **37**, 6153 (2004).
[19] R. L. McSwain, A. R. Markowitz, and K. R. Shull, J. Polym. Sci., Part B: Polym. Phys. **42**, 3809 (2004).
[20] P. Müller-Buschbaum, T. Ittner, and W. Petry, Europhys. Lett. **66**, 513 (2004).
[21] J. C. Grunlan, D. L. Holguin, H.-K. Chuang, I. Perez, A. Chavira, R. Quilatan, J. Akhave, and A. R. Mehrabi, Macromol. Rapid Commun. **25**, 286 (2004).
[22] A. J. Crosby, A. Karim, and E. J. Amis, J. Polym. Sci., Part B: Polym. Phys. **41**, 883 (2003).
[23] A. M. Forster, W. Zhang, A. J. Crosby, and C. M. Stafford, Meas. Sci. Technol. **16**, 81 (2005).
[24] A. J. Crosby, J. Mater. Sci. **38**, 4439 (2003).
[25] Equipment and instruments or materials are identified in the paper in order to adequately specify the experimental details. Such identification does not imply recommendation by NIST, nor does it imply the materials are necessarily the best available for the purpose.
[26] N. Nakajima, R. Babrowicz, and E. R. Harrell, J. Appl. Polym. Sci. **44**, 1437 (1992).
[27] A. Roos and C. Creton, Macromol. Symp. **214**, 147 (2004).
[28] K. Brown, J. C. Hooker, and C. Creton, Macromol. Mater. Eng. **287**, 163 (2002).
[29] A. Zosel, Int. J. Adhes. Adhes. **18**, 265 (1998).